GA–A22489

STABILITY IN HIGH GAIN PLASMAS IN DIII–D

by
E.A. LAZARUS, G.A. NAVRATIL, E.J. STRAIT, B.W. RICE, J.R. FERRON,
C.M. GREENFIELD, M.E. AUSTIN, D.R. BAKER, K.H. BURRELL, T.A. CASPER,
V.S. CHAN, J.C. DeBOO, E.J. DOYLE, R. DURST, C.B. FOREST, P. GOHIL,
R.J. GROEBNER, W.W. HEIDBRINK, R.-M. HONG, W.A. HOULBERG,
A.W. HOWALD, C.-L. HSIEH, A.W. HYATT, G.L. JACKSON, J. KIM, R.J. LA HAYE,
L.L. LAO, C.J. LASNIER, A.W. LEONARD, J. LOHR, R. MAINGI, R.L. MILLER,
M. MURAKAMI, T.H. OSBORNE, L.J. PERKINS, C.C. PETTY, C.L. RETTIG,
T.L. RHODES, S.A. SABBAGH, D.P. SCHISSEL, J.T. SCOVILLE, A.C.C. SIPS,
R.T. SNIDER, F.X. SÖLDNER, G.M. STAEBLER, B.W. STALLARD,
R.D. STAMBAUGH, H.E. ST. JOHN, R.E. STOCKDALE, P.L. TAYLOR, T.S. TAYLOR,
D.M. THOMAS, A.D. TURNBULL, M.R. WADE, R.D. WOOD, and D.G. WHYTE

SEPTEMBER 1996

GA–A22489

STABILITY IN HIGH GAIN PLASMAS IN DIII–D

by
E.A. LAZARUS,[*] G.A. NAVRATIL,[†] E.J. STRAIT, B.W. RICE,[‡] J.R. FERRON, C.M. GREENFIELD, M.E. AUSTIN,[△] D.R. BAKER, K.H. BURRELL, T.A. CASPER,[‡] V.S. CHAN, J.C. DeBOO, E.J. DOYLE,[◊] R. DURST,[¶] C.B. FOREST, P. GOHIL, R.J. GROEBNER, W.W. HEIDBRINK,[§] R.-M. HONG, W.A. HOULBERG,[*] A.W. HOWALD, C.-L. HSIEH, A.W. HYATT, G.L. JACKSON, J. KIM, R.J. LA HAYE, L.L. LAO, C.J. LASNIER,[‡] A.W. LEONARD, J. LOHR, R. MAINGI,[∞] R.L. MILLER, M. MURAKAMI,[*] T.H. OSBORNE, L.J. PERKINS,[‡] C.C. PETTY, C.L. RETTIG,[◊] T.L. RHODES,[◊] S.A. SABBAGH,[†] D.P. SCHISSEL, J.T. SCOVILLE, A.C.C. SIPS,[#] R.T. SNIDER, F.X. SÖLDNER,[#] G.M. STAEBLER, B.W. STALLARD, [‡] R.D. STAMBAUGH, H.E. ST. JOHN, R.E. STOCKDALE, P.L. TAYLOR, T.S. TAYLOR, D.M. THOMAS, A.D. TURNBULL, M.R. WADE,[*] R.D. WOOD,[‡] and D.G. WHYTE[❑]

This is a preprint of a paper to be presented at the Sixteenth IAEA International Conference on Plasma Physics and Controlled Nuclear Research, October 7–11, 1996, Montreal, Canada, and to be published in *The Proceedings.*

[*]Oak Ridge National Laboratory, Oak Ridge, Tennessee.
[†]Columbia University, New York, New York.
[‡]Lawrence Livermore National Laboratory, Livermore, California.
[△]University of Maryland, College Park, Maryland.
[◊]University of California, Los Angeles, California.
[¶]University of Wisconsin, Madison, Wisconsin.
[§]University of California, Irvine, California.
[∞]Oak Ridge Associated Universities, Oak Ridge, Tennessee.
[#]JET Joint Undertaking, Abingdon, United Kingdom.
[❑]INRS — Energie et Materiaux, Varennes, Quebec, Canada.

Work supported by
the U.S. Department of Energy under Contract Nos.
DE-AC03-89ER51114, DE-AC05-96OR22464, W-7405-ENG-48,
and Grant Nos. DE-FG03-86ER53266 and NDE-FG05-86ER5

GA PROJECT 3466
SEPTEMBER 1996

F1-CN-64/A1-2

STABILITY IN HIGH GAIN PLASMAS IN DIII–D

ABSTRACT

Fusion power gain has been increased by a factor of 3 in DIII–D plasmas through the use of strong discharge shaping and tailoring of the pressure and current density profiles. H-mode plasmas with weak or negative central magnetic shear are found to have neoclassical ion confinement throughout most of the plasma volume. Improved MHD stability is achieved by controlling the plasma pressure profile width. The highest fusion power gain Q (ratio of fusion power to input power) in deuterium plasmas was 0.0015, which extrapolates to an equivalent Q of 0.32 in a deuterium-tritium plasma and is similar to values achieved in tokamaks of larger size and magnetic fields.

1. INTRODUCTION

A compact, economical tokamak fusion power plant requires both good energy confinement and magnetohydrodynamic (MHD) stability at high beta. Recent experiments [1–3] have demonstrated greatly improved core confinement in tokamak plasmas with negative central magnetic shear (NCS), while ideal MHD calculations [4–6] predict that a central region with negative shear in the safety factor will enhance plasma stability. (Here $\beta = 2\mu_0 \langle p \rangle / B^2$ is the ratio of plasma pressure to magnetic field pressure, while the magnetic shear is defined as $(2V/q)\,dq/dV$ where q is the tokamak safety factor and V is the volume enclosed by a flux surface.) Earlier studies [7] have also shown the importance of strong discharge shaping in improving plasma stability.

High performance plasmas with negative central shear are an important part of the DIII–D research program toward tokamak concept improvement [8]. Control of the initial current density profile leads to reduction of the ion thermal conduction to neoclassical transport levels, [9,10] correlated with suppression of microturbulence by $\mathbf{E}\times\mathbf{B}$ flow shear [11]. Strong discharge shaping and tailoring of the pressure profile improve the MHD stability of NCS plasmas at high beta, [12] leading to record values of fusion reactivity in DIII–D [13]. These results offer the prospect of reduction in the size and field required for achieving higher gain approaching fusion ignition conditions in a plasma and support the viability of the concept [14] of a smaller, economically attractive tokamak power plant [15] through tailoring of the equilibrium profiles.

2. STABILITY OF NCS PLASMAS

Modification of the current density profile in DIII–D leads to plasmas with enhanced core confinement and strongly peaked pressure profiles. Low power neutral beam injection (NBI) during the initial plasma current ramp produces a target plasma with negative central magnetic shear, [16] which develops a core transport barrier as the heating power is increased. H–mode plasmas have an additional transport barrier near the edge, leading to a broader pressure profile. However, NCS plasmas with an L–mode edge exhibit strongly peaked pressure profiles but invariably disrupt at values

of normalized beta $\beta_N = \beta aB/I \sim 2$, about a factor of two less than the values achieved in H–mode [17,18].

This lower L–mode beta limit is consistent with ideal and resistive MHD stability limits. [12] Ideal n=1 kink mode calculations for strongly shaped plasma cross sections predict significant increases in the stability limits for both β and β^* as the pressure profile becomes broader, accompanied by a large increase in plasma reactivity, as shown in Fig. 1. (The rms-average beta, $\beta^* = 2\,\mu_0 \langle p^2 \rangle^{1/2}/B^2$, is more representative of fusion reactivity.) In contrast, the β^* limit has little improvement with the width of the pressure profile in circular cross-section discharges. The disruption itself is consistent with a related resistive instability lying just below the ideal stability limit. [17,19]

Modification of the pressure profile improves the stability, avoiding disruptions and allowing the discharge to reach significantly higher beta and higher fusion performance. The experimental tool used is the timing of the L-H transition, with the transition to H–mode serving to broaden the pressure profile. The evolution of an L–mode and an H–mode plasma are compared in Fig. 2. Small, controlled changes in plasma shape induce an H–mode transition in one case at 2.1 s, indicated by the edge pressure rise [Fig. 2(c)]. The L–mode case disrupts at about 2.25 s [Fig. 2(a)]. The H–mode plasma continues to increase its stored energy [Fig. 2(d)] and fusion reaction rate [Fig. 2(e)] until a stability limit is reached at $\beta_N = 3.7$. The broadening of the pressure profile after the L–H transition is shown in Fig. 3, where profiles are shown

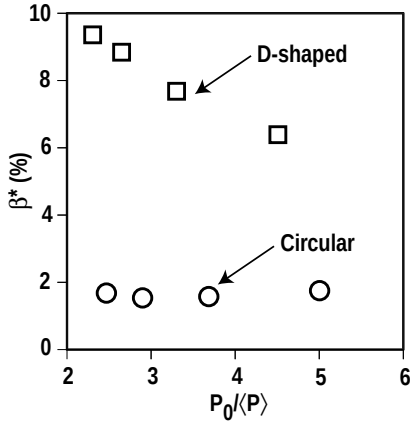

Fig. 1. Maximum β^* (fusion weighted β) stable to the ideal n=1 kink mode vs. pressure peaking factor $p_0/\langle p \rangle$, for profiles of the form $p = p_0 (1 - \rho^2)^\alpha$. Results are shown for a circular cross section and a D-shaped cross setion with elongation 1.7 and triangularity 0.7.

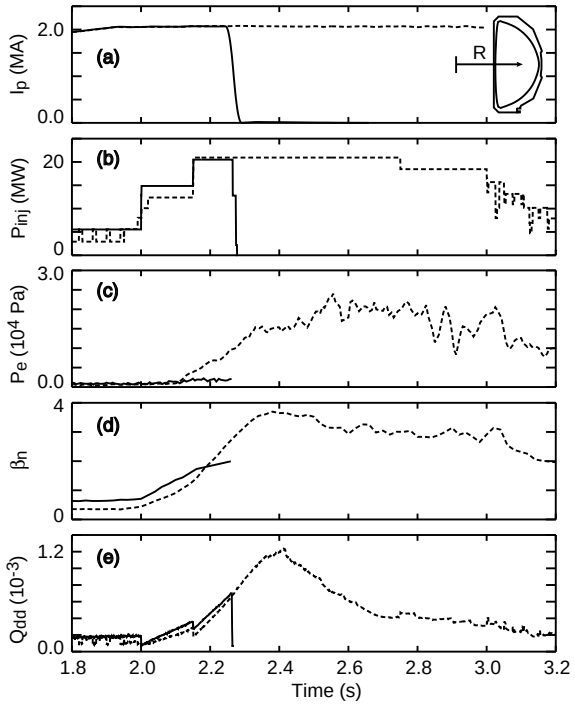

Fig. 2. Time evolution of two similar discharges: 87887 (solid line) which remains in L–mode and disrupts, and 87937 (broken line) which makes a transition to H–mode at 2.1 s. (a) Plasma current, (b) injected neutral beam power, (c) edge electron pressure, (d) β_N (= β a B_t/I_p) in units (% m T/MA), (e) $Q_{dd} = P_{fusion}/P_{NB}$.

just prior to the disruption of the L–mode plasma and 0.125 s after the L–H transition for the H–mode case.

The improved stability with a controlled L-H transition has led to record reactivity for DIII–D plasmas, as shown in Fig. 4 where the D-D fusion neutron rate S_n in discharges with an NCS target phase is plotted against heating power. The L–mode plasmas (solid squares), which typically have pressure peaking ratios $p_0/\langle p\rangle$ in the range 4–5, consistently produce a lower S_n and terminate in a disruption, while H–mode plasmas with $p_0/\langle p\rangle \sim 2$–3 reach much higher S_n. A large shaded circle indicates the discharge with the highest fusion power gain Q (ratio of fusion power to input power), to be discussed below.

The discharges with a broad pressure profile do not typically disrupt, and reach values of β significantly higher than discharges with strong pressure peaking. Eventually they reach stability limits which depend, at least in part, on the form of the q-profile. Figure 5 compares the evolution of the neutron emission, a sensitive indicator of the quality of core confinement, in three discharges with different initial q-profiles. The initial rate of rise of neutron emission in Cases A and B is comparable, indicating similar behavior in the core, while reduced heating power leads to a somewhat slower initial rise in Case C.

Case A (discharge 87953, with strongly negative central shear) suffers a collapse of the central pressure at t = 2.32 s. Earlier, at about t = 2.28 s, this discharge develops a non-rotating n=1 mode near the edge, in the positive shear region. We speculate that this is a consequence of the large current density gradient near the edge, combined with insufficient rotation to maintain wall stabilization. Resistive stability analysis is in progress. The non-rotating mode initially has very little effect on the core plasma and

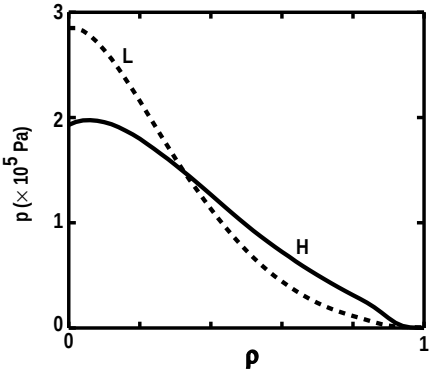

Fig. 3. Pressure profiles for 87887 (L) and 87937 (H) at 2245 ms, showing the broadening of the H–mode vs. ρ, the square root of toroidal normalized flux. The time evolution of these discharges is shown in Fig. 2.

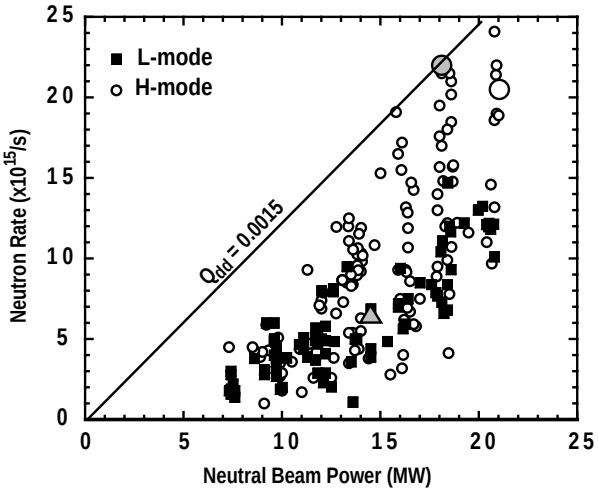

Fig. 4. Results from this experiment displayed as peak neutron rate, S_n, vs. neutral beam power. The solid squares are L–mode plasmas and the open circles are H–mode. The large shaded circle is discharge 87977, discussed in Figs. 5 and 6 and Table I. The large open circle is discharge 87937, shown in Figs. 2 and 3.

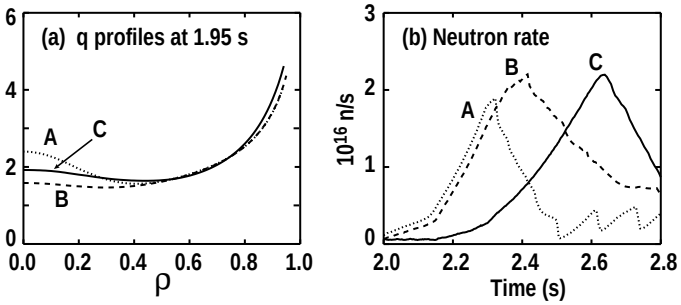

Fig. 5. Comparison of (a) "target" q-profiles before high-power heating and (b) time evolution of the neutron rate, in discharges 87977 (solid line), 87937 (dashed lines), and 87953 (dotted lines).

neutron rate. However, the large stationary island reduces the pressure in the outer part of the plasma leading to a steep pressure gradient in the region of the internal transport barrier. The central collapse is caused by a rapidly growing internal mode, presumably a global resistive mode lying near the ideal stability boundary. The observed internal instability is located in the high pressure gradient region and has a large n=2 component. This is consistent with ideal stability calculations showing that the discharge is stable to n=1, but is marginally unstable to an n=2 kink mode, within the uncertainty of the experimentally measured pressure gradient.

Case B (discharge 87937, also shown as the H–mode case in Fig. 3) has weaker, but still negative, central shear. In this discharge there is no locked mode, but the onset of ELMs at t = 2.32 s leads to mild saturation of the neutron rate and reduction of the edge pressure. The central collapse occurs about 100 ms later than in Case A, after the discharge has reached a higher beta and neutron emission. The collapse is caused by combined internal n=3 and n=2 modes, similar to that of Case A and again near the calculated n=2 ideal stability limit.

Case C (discharge 87977, with highest fusion power gain as discussed below) also has weakly negative central shear with slightly higher central q. It does not have a central collapse but shows a gentle saturation and decline in neutron emission after the onset of ELMs at t = 2.62 s. The ELMs are correlated with MHD instabilities having toroidal mode number n~4, located near the plasma edge. This is in qualitative agreement with ideal high-n ballooning stability calculations which show that the discharge has a broad central region of access to the second stable regime extending over at least half the minor radius, but has reached the first regime stability limit near the edge in the region of the H–mode transport barrier.

The density rise which occurs during H–mode is probably also an important factor in the evolution of these discharges, broadening the neutral beam deposition profile and reducing the central source of energy and momentum needed to sustain the internal transport barrier. Although there is initially no direct effect on discharge performance, this may be the reason that Cases A and B cannot recover from their relatively mild central instabilities. Broadening of the beam deposition may also be the reason for the slow decline of performance in Case C even in the absence of a central instability. The high-triangularity pumped divertor now being installed in DIII–D should make it possible to control the density and maintain central beam deposition in high-performance NCS discharges.

3. TRANSPORT IN NCS PLASMAS

In the discharge with maximum fusion power gain, transport is reduced to neoclassical levels nearly everywhere in the plasma. [9,10] Analysis of discharge 87977 with the TRANSP [20] code shows that the dominant power flow is from the neutral beams to the ions, with the dominant loss terms being convection and collisional transfer to the electron channel. Here we use an effective ion thermal diffusivity $\chi_i^{tot} = Q_i^{tot}/(n_i \nabla T_i)$, avoiding the difficulty of separating the ion heat loss into convective and conductive parts, and in Fig. 6 we compare the experimental χ_i^{tot} to the Chang-Hinton formula [21] for neoclassical diffusivity. This formula is derived in the limit of circular flux surfaces at finite aspect ratio with a correction accounting for an impurity concentration. At a representative time during the L–mode high-power phase (Fig. 6(a)) χ_i^{tot} approaches the neoclassical value in the center of the plasma. A dramatic reduction in ion transport occurs during the H–mode phase [Fig. 6(b)]. At a time near the peak neutron rate and with β in excess of 6%, χ_i^{tot} over the entire plasma is comparable to the neoclassical level. In a more complete treatment using the formulation of Hirshman and Sigmar [22] with the actual equilibrium geometry, the experimentally measured ion heat flux again is consistent with neoclassical predictions [9].

Density fluctuations, measured with far-infrared scattering and beam emission spectroscopy diagnostics, show reductions which correlate well with the observed reduction of the ion transport, suggesting micro turbulence as responsible for the transport. [11] The measured E×B flow shear is sufficient to stabilize ion temperature gradient modes [17], and the large extent of the region of neoclassical level ion transport is consistent with theoretical modeling of suppression of turbulence at high power which can allow a transport bifurcation to develop.[23] In these experiments in DIII–D the E×B flow shear is predominantly driven by toroidal rotation and not the ion pressure gradient.

4. HIGH FUSION GAIN PLASMAS

As shown in Fig. 4, several discharges in these experiments have reached fusion power gains Q_{dd} of about 0.0015. A fusion gain of $Q_{dt} = 0.32$ is projected for a deuterium-tritium plasma under the same conditions as discharge 87977. This estimate of Q_{dt} is obtained from the ratio $Q_{dt}/Q_{dd} = 222$ predicted by simulations using the TRANSP analysis code. No isotopic transport improvements were assumed in the

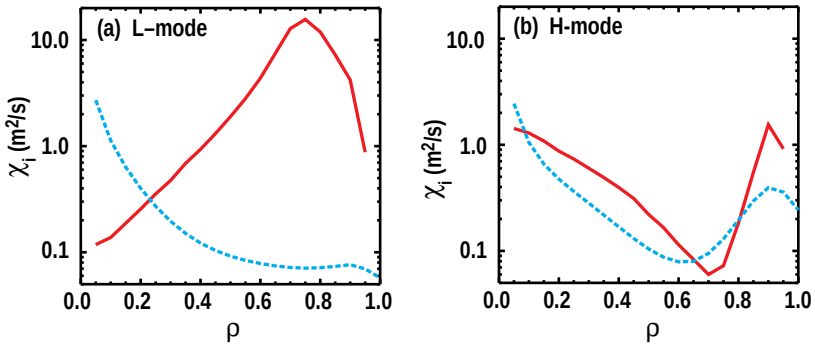

Fig. 6. Ion thermal diffusivity vs. ρ, square-root of the normalized toroidal flux. The solid lines are the experiment and the dashed lines are the calculated neoclassical values. Representative time during (a) the high power L–mode phase and (b) the H–mode phase in discharge 87977.

simulations. The measured profiles of 87977 (temperatures, densities, toroidal rotation) were maintained in the simulation and the deuterium was replaced with a nominal 50:50 mixture of deuterium and tritium. The Q_{dt} value is found to be insensitive to uncertainties in the plasma equilibrium, and the dominant uncertainty in Q_{dd} is the 15% statistical uncertainty in the measurement of the neutron emission rate S_n. The peak value $S_n = 2.2 \times 10^{16}\ s^{-1}$ was measured with a calibrated scintillation counter. Values of $S_n = 2.3 \times 10^{16}\ s^{-1}$ measured with a fission product counter and $S_n = 2.5 \times 10^{16}\ s^{-1}$ from a TRANSP calculation using the measured temperature, density and rotation profiles provide confidence in these results.

For purposes of comparison between tokamaks and extrapolation to future devices, we wish to express Q_{dd} in a way that clearly separates the effects of machine size and field strength from the intrinsic plasma properties of confinement and stability. The fusion gain, Q, is given by

$$Q_{dd} = \frac{1}{2}\frac{\int n_i^2 \overline{\sigma v}\,\xi_r dV}{P_{input}} \cong \frac{\overline{\sigma v}\,\xi_r}{2T_i^2}\ \frac{\langle p^2\rangle}{\langle p\rangle^2}\ \frac{(2\pi R)\pi a^2 \kappa \langle p\rangle^2}{P_{input}\left(1+T_e/T_i\right)^2} \tag{1}$$

For ion temperatures T_i in the range of interest, the fusion reaction rate scales approximately as T_i^2, so $C_f \equiv \overline{\sigma v}\,\xi_r / 2T_i^2$ is approximately constant and the fusion power scales as the square of the plasma pressure. Here the volume is approximated as that of an ellipsoid of revolution. Equation (1) is correct but contains no insight on the relation of Q to tokamak physics. We now describe the plasma geometry by defining an effective inverse aspect ratio E [7,24] in analogy to the usual inverse aspect ratio ε. For diverted plasmas q_{95} is substituted for *q* in the expression for E.

$$\varepsilon = a/R = q_{cyl}\left(\frac{\mu_0 I_p}{2\pi a B}\right) \quad \Rightarrow \quad E \equiv q_\psi\left(\frac{\mu_0 I_p}{2\pi a B}\right) \tag{2}$$

The energy confinement time is expressed as

$$\tau_E = \frac{W}{P_{input} - dW/dt} = \frac{3}{2}\frac{(2\pi R)\pi a^2 \kappa}{P_{input} - dW/dt}\ \frac{\beta B^2}{2\mu_0} \tag{3}$$

A simple scaling for global confinement time in ELM-free H–mode plasmas [25], DIII–D/JET scaling can be approximated as

$$\tau_E = \frac{W}{P_{input} - dW/dt} = 1.1 \times 10^{-4} \cdot H_{JD}\frac{I_p R^{3/2}}{\sqrt{P_{input} - dW/dt}} \tag{4}$$

(in SI units) where H_{JD} is an enhancement factor over the original scaling. Combining the above relations we find

$$Q_{dd} = 1.2 \times 10^{-8}\left[\frac{8C_f}{9\mu_0^2\left(1+T_e/T_i\right)^2}\right] B^2 R^2 \left[\frac{\beta^*}{\beta}\right]^2 \left[\frac{E}{\sqrt{\kappa}\,q}\right]^2 H_{JD}^2. \tag{5}$$

The quantity B^2R^2, proportional to the square of the center post current, represents the stress limit in tokamak construction. The shaping factor E is related to n=0 stability, [24] while q and the pressure profile peaking factor, (β^*/β), are related to n=1 stability. In DIII-D, the quantity $(\beta^*/\beta) \cdot (E/q\sqrt{\kappa})$ appears to reach values quite close to the ideal MHD stability limitation. The confinement scaling and the enhancement factor, H_{JD}, are strictly empirical.

To demonstrate more clearly how these results extrapolate to requirements for achieving higher gain approaching fusion ignition conditions in a plasma, we separate the parametric dependence of Q_{dd} on primarily economic and technological factors, B^2R^2, from the dependence on dimensionless plasma parameters, $[(\beta^*/\beta) \cdot (E/q\sqrt{\kappa})H_{JD}]^2$. Calculations similar to those in Ref. [15], with the reactor design systems code (SuperCode) show that the capital cost of the tokamak reactor core increases approximately linearly with B^2R^2. As shown in Fig. 7, the simple expression for $Q_{dd}/(BR)^2$ given by Eq. (5) is adequate to describe the highest performance plasmas in several other tokamaks. [26,27,28] For purposes of comparison with other published values we have plotted $Q^*_{dd} \equiv P_t/(P_{NBI} - W) + (P_{bt} + P_{bb})/P_{NBI}$, where P_t, P_{bt}, and P_{bb} are the fusion powers from thermal-thermal, beam-thermal, and beam-beam reactions respectively. Here both the thermonuclear fusion reaction rate and the energy confinement time are referenced to the input power which would be required to sustain the plasma's thermal energy in steady state. Details such as impurity concentration, individual form factors for temperature and density profiles, T_i/T_e, the thermal fraction of fusion power, and neutral beam deposition profile are sufficiently similar to be ignored. Additionally, all are free of sawteeth because of the current profile. The confinement factor, H_{JD}, is determined from the experimental data and no predictive capability is implied. The relative importance of the individual terms in the abscissa is shown in Table I.

Normalized to B^2R^2 the fusion gain results reported here are between 2 and 9 times larger than those achieved in other tokamaks, primarily as a consequence of strong shaping and enhanced confinement. As shown in Table I, DIII–D has smaller B and R than the other tokamaks listed, but this is counterbalanced by the strong shaping

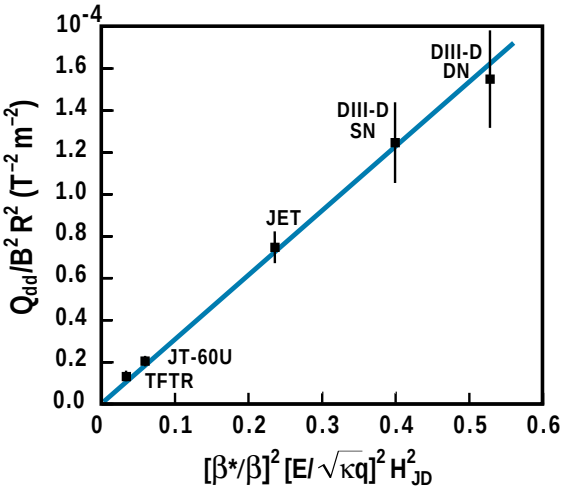

Fig. 7. Q^*_{dd} vs. scaling relation discussed in the text for the highest DIII–D Q_{dd} and the highest values reported by TFTR, JET, and JT-60.

TABLE I. Comparison of D-D fusion reactivity for several tokamaks.

Tokamak	DIII–D (double-null)	DIII–D (single-null)	TFTR [28]	JT-60U [27]	JET [26]
Discharge #	87977	88964	68522	17110	26087
B (T)	2.15	2.15	5.00	4.40	2.80
R (m)	1.67	1.69	2.50	3.05	2.95
$E/\kappa^{1/2}$	0.98	0.76	0.35	0.39	0.60
H_{JD}	2.4	2.6	1.2	1.8	2.3
q	4.2	3.7	3.8	4.0	3.8
τ_E(s)	0.40	0.43	0.19	0.54	1.30
β (%)	6.7	5.8	1.0	1.5	2.2
$<p^2>/<p>^2$ (a)	1.6	1.3	3.0	2.0	1.8
Q_{dd}^*	0.0020	0.0016	0.0021	0.0037	0.0051

(a)Estimated from the ratio of peak to average pressure. A radial profile of the form $p(\rho) \propto (1-\rho^2)^\alpha$ is assumed, yielding $\alpha = p_0/<p>-1$ and $f_{p=} <p^2>/<p>^2 = (\alpha+1)^2/(2\alpha+1)$.

and associated enhanced confinement which allow it to operate at higher beta with modest input power.

Low-triangularity single-null DIII–D discharges with negative central shear [29] are also consistent with the scaling for Q_{dd}. The discharge shape and profiles are shown in Fig. 8. These discharges extend the regime of neoclassical core confinement associated with negative or weak central magnetic shear to plasmas with the low safety factor ($q_{95} \sim 3.3$) and triangularity ($\delta \sim 0.3$) anticipated in future tokamaks such as ITER. Energy confinement times exceed the ITER–89P L–mode scaling law by up to a factor of 4, and are almost twice as large as in previous single-null cases with $3 \le q_{95} \le$

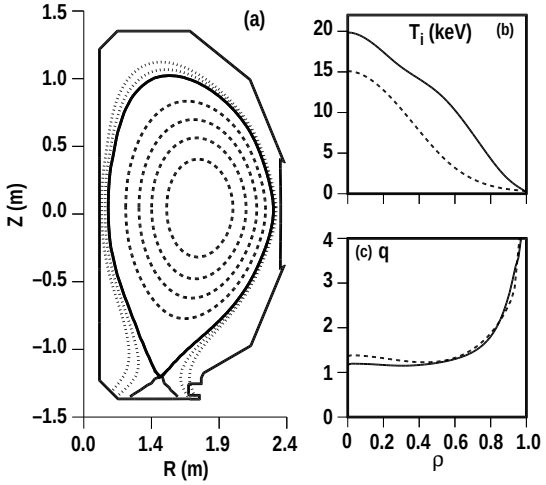

Fig. 8. High performance single-null plasma with negative central shear (88964), showing (a) the plasma shape with (b) T_i and (c) q profiles at times with an L–mode edge (broken lines, t = 2.1 s) and an H–mode edge (solid lines, t = 2.4 s).

4. The normalized beta [β (aB/I)] reaches values as high as 4, comparable to the best previous single-null discharges, with no confinement deterioration. The peak fusion power gains of $Q_{dd} = 1.0 \times 10^{-3}$ and D-D neutron rates of 1.4×10^{16} s^{-1} are more than double the previous maximum values for single-null discharges. Although high triangularity allows a larger plasma current and theoretically a higher β-limit, the fusion gain in these low triangularity plasmas is similar to that of high triangularity double-null plasmas at the same plasma current. These results are favorable for advanced performance operation in ITER, JT-60U and for D-T experiments in JET; high performance experiments in deuterium NCS plasmas have recently begun in JET with encouraging results [30].

5. CONCLUSIONS

In conclusion, control of the pressure profile has been accomplished by selective timing of the L-H transition. The resulting increase in β^* is consistent with expectations based on ideal MHD stability calculations. The plasmas exhibit a neoclassical level of ion transport in the core during the L–mode phase and this level extends over the entire plasma cross-section after the L-H transition. Negative magnetic shear early in the discharge appears to be a necessary condition in achieving good core confinement. However, later in the discharge other mechanisms are responsible for transport reduction, and the details of the shear profile become less important to the ion transport. The highest-performance plasmas evolve to a weakly negative or weakly positive shear in the central region. Plasmas with increased shear reversal show similar ion transport but reduced stability in that they collapse at lower β^*. The improved stability and confinement has allowed DIII–D to achieve a fusion gain in deuterium plasmas of $Q_{dd} = 0.0015$, which extrapolates to $Q_{dt}^{equiv} = 0.32$ in a deuterium-tritium mixture. The Q_{dd} is comparable to that achieved in larger tokamaks with higher magnetic fields.

REFERENCES

[1] HUGON, M., *et al.*, Nucl. Fusion **32** 33 (1992).
[2] STRAIT, E. J., *et al.*, Phys. Rev. Lett. **75** 4421 (1995).
[3] LEVINTON, F.M., *et al.*, Phys. Rev. Lett. **75** 4417 (1995).
[4] SYKES, A. and TURNER, M. F., in Proc. Euro. Conf. on Contr. Fusion and Plasma Phys., Oxford, 1979 (EPS, Petit-Lancy, Switzerland).
[5] TURNBULL, A. D., *et al.*, Phys. Rev. Lett. **74** 718 (1995).
[6] KESSEL, C., *et al.*, Phys. Rev. Lett. **72** 1212 (1995).
[7] LAZARUS, E. A., *et al.*, Phys. Fluids B **3** 2220 (1991).
[8] CHAN, V. S., *et al.*, F1-CN-64/O1-6 this conference.
[9] LAZARUS, E. A., *et al.*, Phys. Rev. Lett. **77** 2714 (1996).
[10] SCHISSEL, D., *et al.*, F1-CN-64/A5-3 this conference.
[11] DOYLE, E. J., *et al.*, F1-CN-64/A6-4 this conference.
[12] TURNBULL, A. D., *et al.*, F1-CN-64/DP-1 this conference.
[13] LAZARUS, E. A., *et al.*, "Higher fusion power gain with profile control in DIII-D tokamak plasmas," to be published in Nucl. Fusion.
[14] TAYLOR, T. S., *et al.*, Plasma Phys. Control. Fusion **36** B229 (1994).
[15] GALAMBOS, J. D., *et al.*, Nucl. Fusion **35** 551 (1995).
[16] RICE, B.W., *et al.*, Plasma Phys. Control. Fusion **38** 869 (1996).
[17] LAO, L. L., *et al.*, Phys. Plasmas **3** 1951 (1996).
[18] RICE, B.W., *et al.*, Phys. Plasmas **3** 1983 (1996).

[19] CHU, M. S., *et al.*, Phys. Rev. Lett. **77** 2710 (1996).
[20] GOLDSTON, R.J., *et al.*, J. Comput. Phys. **43** 61 (1981).
[21] CHANG, C.S., and HINTON, F.L. , Phys. Fluids **29** 3314 (1986).
[22] HIRSHMAN, S.P., and SIGMAR, D.J. , Nucl. Fusion **21** 1079 (1981).
[23] STAEBLER, G.M., *et al.*, Phys. Plasma **1** 99 (1994).
[24] LAZARUS, E.A., *et al.*, Phys. Fluids B **4** 3644 (1992).
[25] SCHISSEL, D.P., *et al.*, Nucl. Fusion **31** 73 (1991).
[26] JET TEAM, Nucl. Fusion **32** 187 (1992).
[27] NISHITANI, T., *et al.*, Nucl. Fusion **34** 1069 (1994).
[28] HAWRYLUK, R.J., *et al.*, Plasma Physics and Controlled Nuclear Fusion Research 1994 (IAEA, Vienna, 1995), Vol. 1, p . 11.
[29] STRAIT, E. J., *et al.*, in Proc. 23rd Euro. Conf. on Contr. Fusion and Plasma Phys. (EPS, Petit-Lancy, Switzerland, 1996) to be published.
[30] GORMEZANO, C., *et al.*, IAEA-CN-64/A5-5, this conference.